NUMERICAL STUDY OF JET INTERACTION AT SUPER- AND HYPERSONIC SPEEDS FOR FLIGHT VEHICLE CONTROL

J. Brandeis
RAFAEL
POB 2250
Haifa, Israel

Abstract

A numerical, two-dimensional study of the jet interaction is presented. Emphasis is placed on optimization of the aerodynamic control force by examining in detail the force amplification parameters. The investigation first covers flat plates with slot-injection of sonic jet. For this configuration much experimental data exists and it is used to validate the present numerical simulations. The parameters investigated are the jet injection pressure, the free stream Mach number, and the angle of injection. The initial transient solution during which the interaction flow field is formed, is also presented. The effect of the ogival an elliptic nose shapes having attached and detached shock waves, on the jet interaction is studied. The shock significantly affects the jet induced flow field, but the force amplification factors were surprisingly similar to the flat plate results.

1. GENERAL

The transverse injection of a jet into an external stream is an attractive alternative for flight vehicle control. There are several reasons that make this method an appealing means for affecting control of hypersonic flight vehicles. First, with jet impulse control external control surfaces that generate drag and heat can be dispensed with. The method of jet injection carries with it no appreciable drag penalty. It is mechanically simple (few if any moving parts) and does not require mechanical actuators and the associated power supply. Its limiting parameters on the other hand are large working pressures and internal temperatures, if combustible source is used. Fluidic switching is still a technological challenge.

The use of such jet thrusters for vehicle control is especially attractive in hypersonic flow as it takes advantage of the jet interaction phenomenon to increase significantly the available control force. At supersonic and hypersonic speeds, the jet injected normally into the outer flow, gives rise to a significant upstream separation of the boundary layer, which causes a significant rise in surface pressure. The integrated pressure gives a force that acts in the same direction as the jet thrust and is of comparable magnitude. At subsonic speed, by contrast, the interaction effects do not lead to such force amplification, and may actually be detrimental.

The jet interaction problem has additional applications that make it of great interest to researchers. One of the critical componenets of a SCRAM (Supersonic Combustion Ram) jet engine is the injector. Here, the fuel (liquid or gas) is injected into a supersonic stream. Proper mixing of fuel and oxidizer must be assured for the SCRAM jet to operate.

In this study the jet interaction is examined strictly as a device for enhancing the control force available for vehicle steering. Only injection into the external high speed flow is considered. The treatment is numerical and is limited to planar configurations. However, transient effects and multispecies hot flows were considered. Special emphasis is placed on estimating the force amplification due to the jet interaction and how it is affected by various body shape and injection geometry parameters. For this purpose, a parametric investigation was made computationally. The two dimensionality of the flow makes the analysis and comparison with experiments simpler. Also, a similar three-dimensional work would have to be very limited in scope due to prohibitively large CPU requirements even on the most advanced supercomputer. It is hoped to use the numerical results for generating information useful for engineering design.

Most previous computational works reported in literature relate to general flow simulation and aim at configuration design and code validation. These are often extensive, three-dimensional computational efforts, and therefore understandibly few cases can be computed. Impressive computational results for the three-dimensional jet interaction were presented by Shang et al. [1] and McMaster et al. [2]. They quote a typical run time as 40 hrs on CRAY 2. Noteworthy also are the computations carried out by Lombard et al. [3,4] using an efficient supra-characteristics method for simulating the use of impulse control on HEDI interceptor. Experimental results for two-dimensional jet interaction flow field and pressure distribution have been available for many years [5,6], and were used for comparison with the present computations.

2. THE COMPUTATIONAL METHOD AND NUMERICAL CONSIDERATIONS

The computational method employed in this study is the PISCES [7] computer code. This is a two-dimensional (and axisymmetric) finite difference, explicit computer program used widely for studying fluid-structure interaction. For the present study, the Navier-Stokes equations are solved using a second-order accurate, finite volume scheme. The solution is time accurate and multiple species are allowed. The numerical solution is carried out on a block-structured grid where the grid density may be controlled to obtain good resolution where needed. This feature is especially important since the total number of points is limited. The no-slip boundary condition is used at the wall together with the Cebeci-Smith turbulence model. For inflow, the fluid properties, including en-

ergy are specified. Outflow conditions are of Neumann type. Since this is a time-dependent calculation, the performance of the code is measured by examining the conservation of mass, momentum, energy, etc. within the domain during the run. Convergence to steady-state is assumed when the separation point location reaches a steady value.

The size of the computational domain for all cases considered here was 100 cm x 20 cm, and 90 x 36 (or 100 x 50) grid points were used. The grid points were clustered around the injection slot (1.2 cm in width) and around other regions where good definition was required. For example, about 15 points were used to define the boundary layer and six grid points were used to span the injection slot. The finest spacing (0.2 cm x 0.074 or 0.02 cm) was, therefore, in the injection region, for nominal Reynolds numbers based on the free stream conditions and length to the injection port, of $O(10^7)$. An effort was made to investigate the sensitivity of solution to grid density by increasing the number of grid points up to the maximum (100x50) and at the same time also increasing the local grid density in the region of interest by a factor of two. The control parameter showed a sensitivity of less than 5% to these changes. Since this is a comparative study, the present grid structure was judged to be adequate. Since this is an explicit method, and numerous runs were made, a more refined grid than that used was not feasible. For the cases where different forebody shapes were considered, the grid was so structured as to allow reasoble definition within that region.

The cases were run until the upstream separation point approached a constant value, which was taken as an indication of reaching a steady state. All results presented here achieved steady state. The computations were carried out on a Convex 210 computer. The typical CPU time required to reach steady state was 1 ms/grid point/cycle, which translated to 10-20 hrs to reach steady state.

3. THE JET INTERACTION FLOW FIELD AND NUMERICAL METHOD VALIDATION

The experimental results of Spaid [5] regarding the two-dimensional Jet Interaction flow field are still an authoritative base for comparisons. In the present research an attempt was made to simulate some of these experiments. The sketch of the flow field in Figure 1 identifies the major features of the supersonic flow topology. The large separation region ahead of the injected sonic jet has typically two circulation cells. The boundary layer separates ahead of the jet and a significant high pressure region forms exerting a force on the plate in the same direction as the jet thrust. The downstream recirculation region gives rise to lower than ambient pressures in supersonic flow, but in hypersonic flow these pressures are always higher than ambient. The exit static pressure, mass flow rate and thrust for a sonic jet are linked to the jet stagnation pressure by the following relations:

$$P_e = P_{oj}\left(\frac{2}{\gamma+1}\right)^{\frac{\gamma}{\gamma-1}} = 0.528 \ \textit{in air}$$

$$\dot{m} = \rho_e A_e U_e$$

$$T = \dot{m}U_e + (P_e - P_{inf})A_e$$

Poj refers to the jet stagnation pressure, A_e, U_e, ρ_e are the jet exit area, velocity and density, γ is the ratio of specific heats, while Pinf is the ambient static pressure.

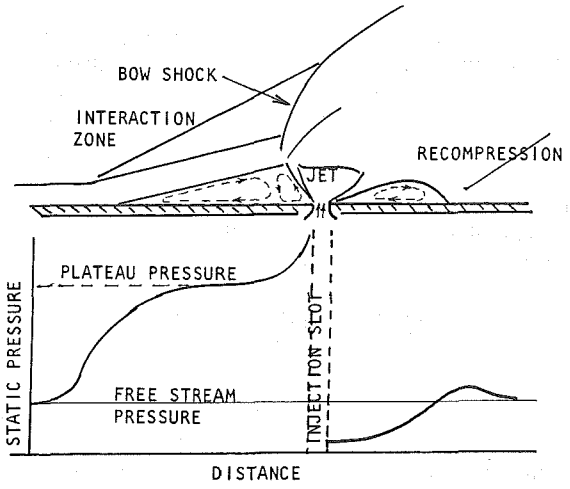

FIG 1. SKETCH OF THE FLOW FIELD

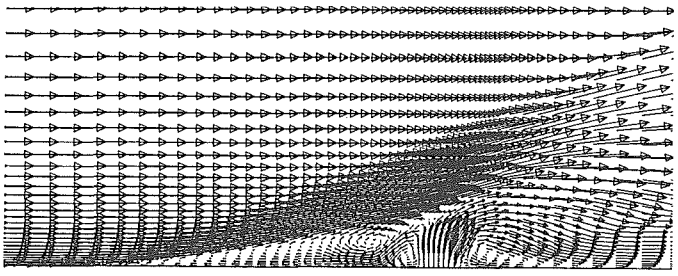

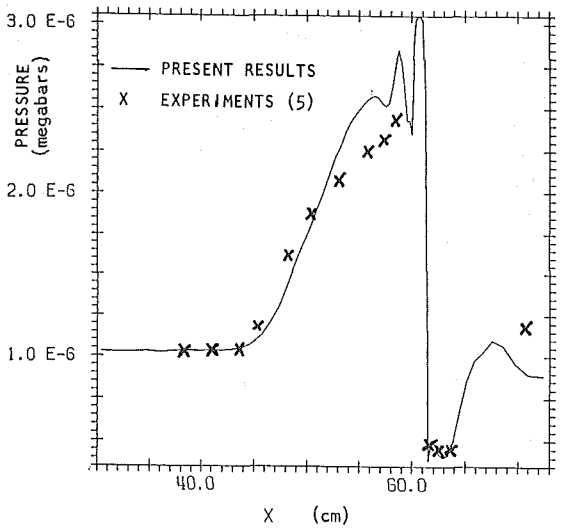

FIG 2. COMPUTED RESULTS FOR Poj/Pin=5.7, Minf=3.5, RE=4x10^7 AND COMPARISON WITH EXPERIMENT (RE=3x10^8)

In Figure 2, a comparison is shown between the present results and experiment [5] for a case where Minf=3.5 and Poj/Pinf=5.7. The Reynolds number for the present simulation is 4x10^7, while in the experiment it is 3x10^8. This disparity should be unimportant, as the flow was found to be insensitive

to Reynolds number in the experiments. The free-stream to jet momentum ratio, which is an important parameter, is identical in the two cases compared.

The numerical simulation reproduces faithfully all the flow features identified in the experiment, including the two counter-rotating vortices within the upstream separated region and the shock structure in the overexpanded plume. The detailed surface pressure plots show a good quantitative agreement between the computed and measured results. There is some pressure oscillation in the computed results in the vicinity of the shock, but this is difficult to avoid and appears in other numerical results (for example, refs. 1,2,3).

4. PARAMETRIC STUDIES USING FLAT PLATE GEOMETRY

In this section the results of parametric, numerical studies are reported. The geometry and grid structure were kept constant for groups of cases of the same kind to facilitate comparisons. Where possible, comparisons are drawn with experimental results.

4.1 PRESSURE RATIO EFFECT

Results are presented at Minf=3.5 for the three values of jet stagnation pressure: Poj/Pinf=5.7, 26, 49. It is noted that the jet momentum increases with increasing pressure ratio. The ratio of the jet pressure to external static pressure governs the degree of overexpansion of the jet and thus influences the penetration height, H, which is the distance that the jet penetrates into the outer flow, measured to the Mach disk (where the jet flow turns). The effect of expansion on the structure of the jet flow and the surface pressures can be seen by comparing the upper part (Poj/Pinf=26) of Figure 3 with the results for Poj/Pinf=5.7 in Figure 2. From integrating the surface pressures and calculating the jet thrust, the force amplification parameters can be obtained for comparing the results. The thrust was defined earlier, and is seen to be composed of the mass flux term and a pressure term. The amplification factor, K, is usually defined [5] as

$$K=(Fi+T)/Tsv$$

where Fi is the interaction force obtained from the upstream pressure integration, T is the jet thrust and Tsv is the vacuum thrust of the sonic obtained by equating the ambient pressure in the pressure term of the equation for thrust, to zero. Sometimes it may be convenient to use the direct ratio of interaction force to jet thrust as a measure of performance.

Poj/Pinf	K	Fi/T	$\dot{m}$ [kg/s/m]
5.6	2.9	2.2	15.1
26	2.4	1.3	68.9
49	1.8	0.7	130.4

TABLE 1. INTERACTION PARAMETERS AS FUNCTION OF PRESSURE RATIO. SEA LEVEL, Minf=3.5

The quantitative results are listed in Table 1. It is clearly seen that for the first three cases computed at identical outer flow conditions, the value of the amplification factor decreases with the increase in jet stagnation pressure. The ratio Fi/T at Poj/Pinf=49 is only 30% of that for Poj/Pinf=5.7, while the fuel expenditure (the mass flux) is eight times as great, as is the thrust. There may, in principle, be an optimum operating condition for obtaining the desired total control force while minimizing the fuel expenditure.

4.2 FREE STREAM MACH NUMBER EFFECT

The effect of the free stream Mach number on the jet interaction is now examined. Results for the three representative cases: Minf=3.5, 5.0 and 8.5 are presented, all three for the same (sea level) initial flow conditions and with the pressure ratio for the sonic jet Poj/Pinf=26. These three Mach numbers were chosen because they fit into the supersonic - low hypersonic speed range that is of interest for low altitude applications. The velocity vector plots for these cases appear in Figure 3. Several qualitative results are immediately noted from these plots. First, the penetration height decreases with Mach number as may be expected because the jet to cross flow momentum ratio $(pU^2)j/(pU^2)inf$ also decreases. The momentum ratio is a measure of relative momentum of the two interacting streams and is a dominant parameter affecting the penetration height [5,6,8]. The upstream separation distance is in turn proportional to the effective obstacle height (penetration height, H). The shape of the jet plume is preserved, as would be expected considering that the jet pressure is the same for all three cases.

The wall pressure distributions for the three Mach numbers are shown in Figure 3. It is evident that the separation zone shrinks with Mach number, while the pressures increase. The pressure in the region where it is almost invariant with distance is called the plateau pressure. A correlation relating these plateau pressures to the Mach number was given by Zukoski [8] based on experimental data is

$$Pplat/Pinf=1+Minf/2.$$

The present computed results are shown together with the correlation formula (the straight line) in Figure 4. It is seen that the results fit the correlation formula rather well except for the Minf=8.5 case where there is a large overshoot. It is noted that a similar experimental comparison due to Spaid [5] shows good correlation for Minf<6, but a wide spread of data was obtained for the hypersonic Mach numbers. It is therefore difficult to say if the present Minf=8.5 result is discrepant. A note is made that there are no experimental results for sea level conditions.

The interaction parameters for this group of cases are listed in Table 2. There appears to be a direct relation between the amplification factor and Mach number indicating that larger interaction force is generated at higher speeds. Eperimental data [5] shows general insensitivity to Mach nuber. There is a considerable spread of data, 2<K<3.5, and the

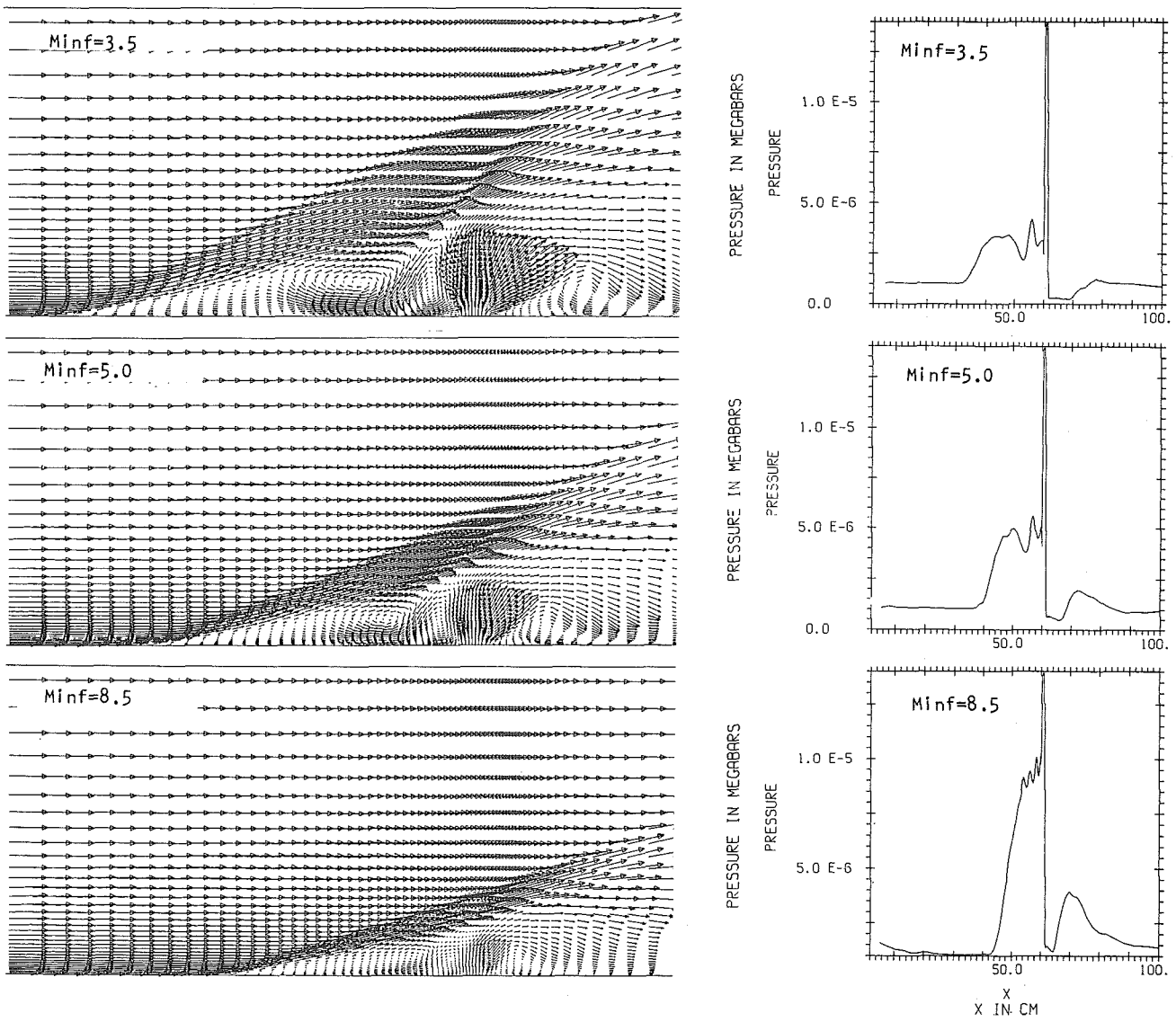

FIG 3. VELOCITY VECTOR PLOTS AND SURFACE PRESSURES FOR THREE MACH NUMBERS. Poj/Pinf=26.

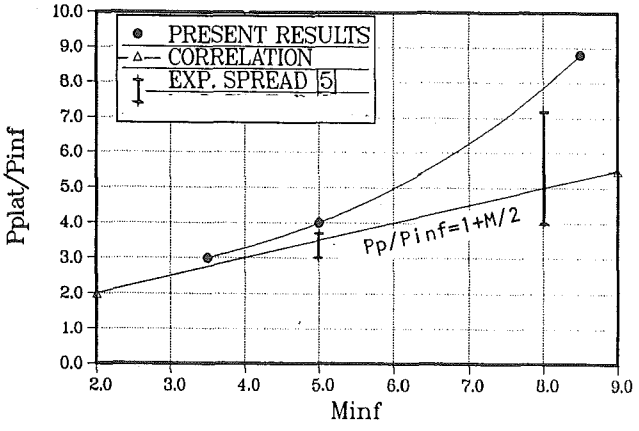

FIG 4. VARIATION OF PLATEAU PRESSURE WITH MACH NUMBER - COMPUTED VS. EXPERIMENTAL.

present results fit nicely within this range. Lastly, it is noted that the downstream pressures behave as observed in experiments: at supersonic speeds the pressures downstream of the injection port show a drop below ambient, while at hypersonic speed they are always higher [5] (see Figure 3, Minf=8.5).

Minf	K	Fi/T	$\dot{m}$ [kg/s/m]
3.5	2.5	1.4	68.9
5.0	2.9	1.8	68.9
8.5	3.2	2.1	68.9

TABLE 2. INTERACTION PARAMETERS AS FUNCTION OF MACH NUMBER. SEA LEVEL, Poj/Pinf=26

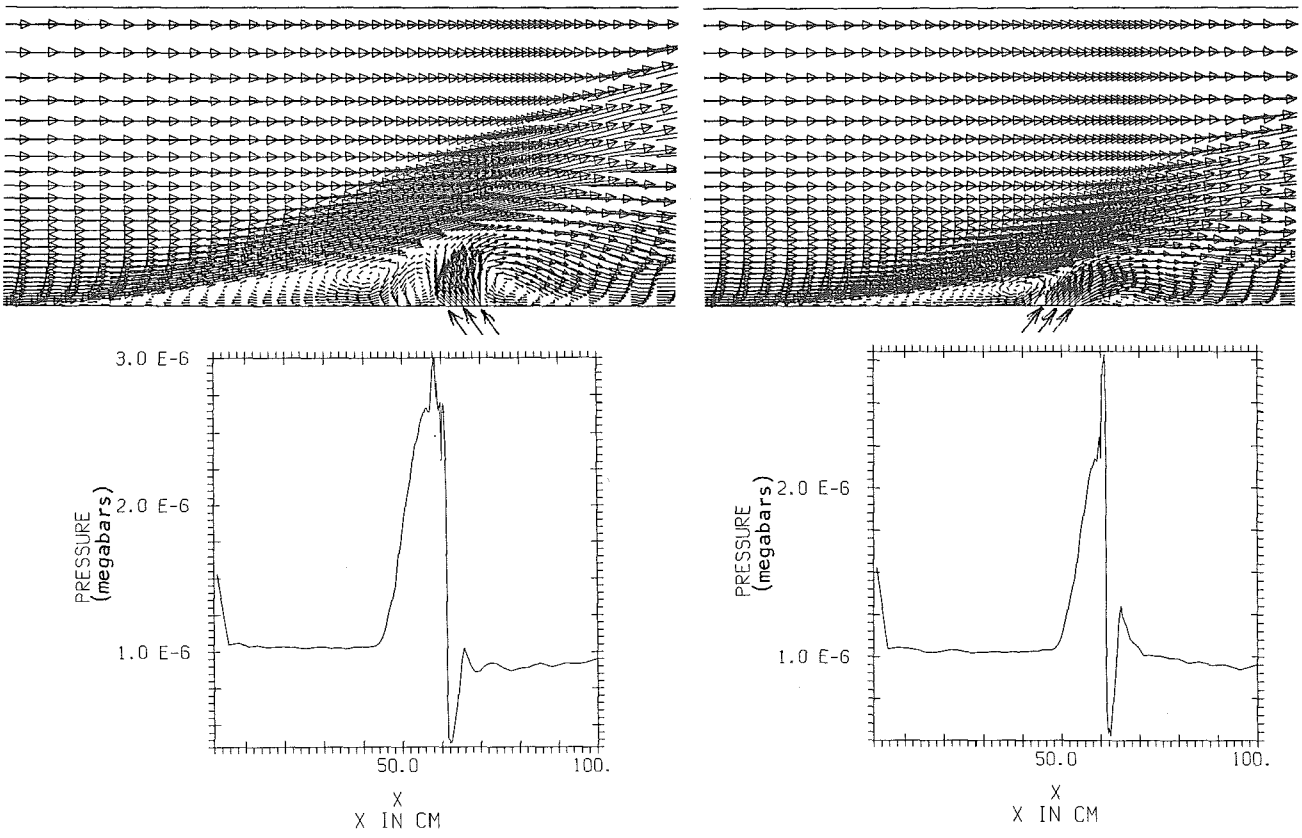

FIG 5. VELOCITY VECTOR PLOTS, AND SURFACE PRESSURES FOR UPSTREAM-VECTORED INJECTION (LEFT) AND FOR DOWNSTREAM-VECTORED INJECTION (RIGHT). Poj/Pinf=5.7, Minf=3.5

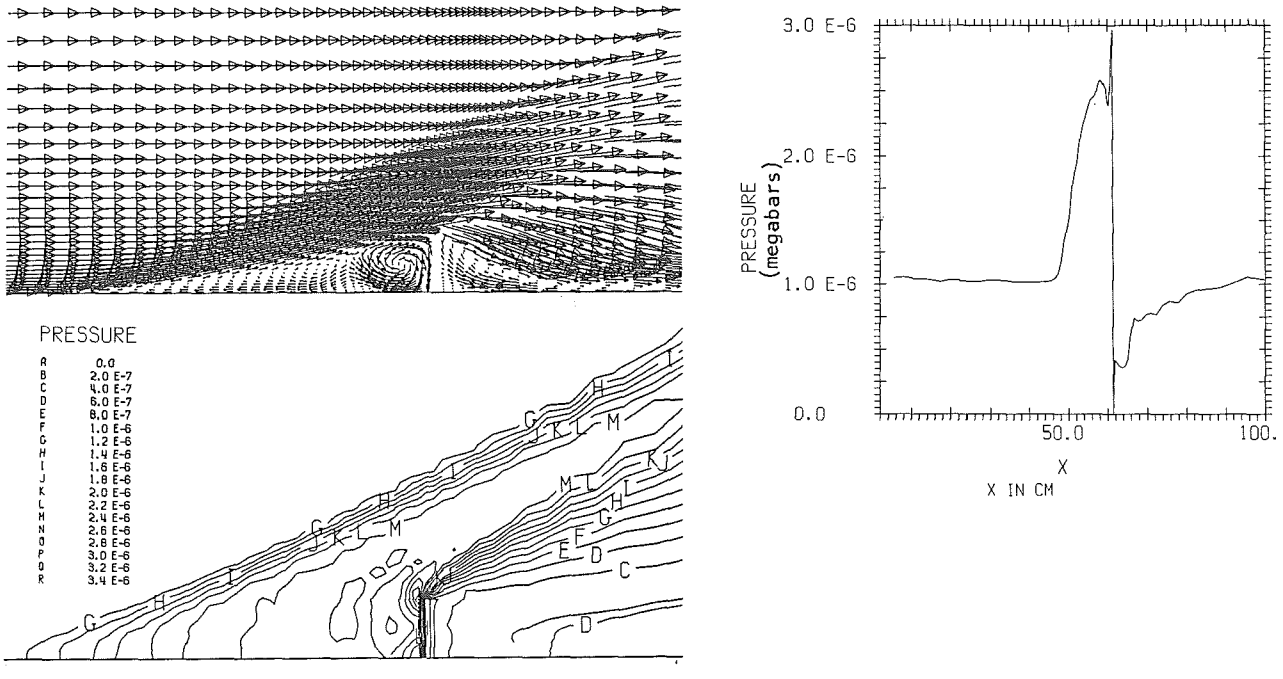

FIG 6. VELOCITY VECTOR PLOT, EQUAL PRESSURE CONTOURS AND SURFACE PRESSURE FOR THE 2 cm HIGH SPOILER. Minf=3.5

4.3 INJECTION ANGLE EFFECT

Next, the influence of vectoring the injected jet is considered. Simulations were carried out for two injection angles (in addition to the standard case of injection normal to the plate): one, inclined in the direction of the flow at 45 degrees, and the second at 45 degrees against the flow direction. Two injection pressure ratios were considered to test the influence of jet expansion. The flow field and surface pressures comparing the two cases at the lower injection pressure are shown in Figure 5. It is seen that the upstream separation is much more extensive for the case where the jet is directed at 45 degrees against the free stream. The separation zone is considerably longer and the plateau pressure is higher. Two large counter rotating vortices are identified, and there is a third, minor, cell at the leading edge of the injection slot. The downstream vortex is also more pronounced for this case.

Before analysis is made of the interaction parameters, as done in the two previous cases, the definitions for thrust is taken for consistency to include the total thrust force along the injection axis and not just the component normal to the surface. This is done in order to facilitate comparison with other cases. With this in mind, the quantitative results are listed in Table 3. Comparing the three cases for the injection pressure ratio of 5.7 it is seen that considerable increase in control force amplification is derived by injecting against the main flow direction. By contrast, injection in the downstream direction greatly decreases the interaction force. Similar findings were made experimentally [9] using water jet injection into a supersonic air flow.

The same general trend is obtained from the comperison between upstream and normal injection with Poj/Pinf=26, having more extensive plume overexpansion. The relative advantage of vectoring the jet upstream is much smaller, even marginal, for this case. The effect of plume overexpansion, and hence the penetration height, in reducing the length of the interaction zone for the upstream vectored jet, is seen. It appears, therefore, that upstream vectoring of the jet offers a distinct advantage when the plume expansion ratio is small.

ANGLE[deg]	Poj/Pinf	K	Fi/T	$\dot{m}$[kg/s/m]
0	5.7	2.9	2.2	15.1
-45	5.7	3.9	3.0	15.1
+45	5.7	2.1	1.1	15.1
0	26	2.5	1.4	68.9
-45	26	2.9	1.6	68.9

TABLE 3. INTERACTION PARAMETERS AS FUNCTION OF INJECTION ANGLE. (- for upstream, + for downstream). SEA LEVEL, Minf=3.5

5. ANALOGY WITH MECHANICAL SPOILER

The transverse jet injection for vehicle steering is sometimes referred to as jet spoiler because of the analogy between the two flow fields from the point of view of the upsteam interaction. An attempt is made to show the aerodynamic advantage of the jet as compared to the spoiler which is a mechanical obstruction to the flow. The spoiler is modeled for the purpose of the simulation as a variable height wall (a thin column of cells on the mesh) which is clearly analogous to the jet penetration height described earlier. The flow-field velocity vectors plot, pressure map and wall pressure distribution for spoiler 2 cm. in height, appears in Figure 6. This should be compared with the results for jet with pressure ratio of 5.7 in Figure 3. The qualitative analogy between the two flows is clearly seen. Both flows produce an upstream overpressure region. However, for the spoiler there is no thrust force but there is a considerable drag penalty. The relevant results are listed in Table 4. The drag force was obtained by direct force integration over the entire surface of the spoiler.

It is seen from Table 4 that the drag of the spoiler is proportional to its height, as expected. More significantly, drag as a percentage of the interaction force also increases with the spoiler height, at least for the two cases considered. For the 2cm. high spoiler, the drag is 40% of the interaction force generated. This is a severe penalty from the design stand point. By contrast, jets generate no such drag. Roughly, the jet with pressure ratio of 5.7 generates an interaction force similar to the 2cm. spoiler.

CASE	Fi[nt/m]	DRAG[nt/m]	Fi/DRAG
SPOILER 1cm	68.2	19.5	3.5
SPOILER 2cm	156.3	60	2.6
JET Poj/Pinf=26	502.8	-	-
JET Poj/Pinf=5.7	145.5	-	-

TABLE 4. FORCE RESULTS FOR SPOILER AND JET. SEA LEVEL, Minf=3.5

6. TRANSIENT RESPONSE

In the actual application as steering motor, the thruster is activated for short duration pulses or discrete pyrotechnic charges are used. The activation time is usually a fraction of a second. Therefore, thrust build-up and creation of the interaction flow field are very relevant problems, warranting examination. Computational data was obtained for three flat plate simulations, at early stages of the flow field formation. The ambient conditions were Minf=3.5 at standard sea level, and two jet pressure ratios: 26 and 48 were used. In one case (Poj/Pinf=26) a shear layer profile was assumed at inflow to simulate a very thick boundary layer (approximately three fold increase in thickness).

The length of the interaction region, X, and the ratio X/H, where H is the penetration height, are plotted versus time in Figures 7 and 8, respectively. For all three cases the interaction region reaches quickly most of its fully developed length, but completes its growth asymptotically. Most of this growth takes place during the time it takes for the outer flow to traverse the interaction length, X (~0.25ms in the present problem). For the two cases with normal boundary layers the ratio

X/H reaches its maximum even faster, and then remains constant for the remainder of the formation process. For the case where the approaching boundary layer is a relatively thick shear layer, this behavior is not observed.

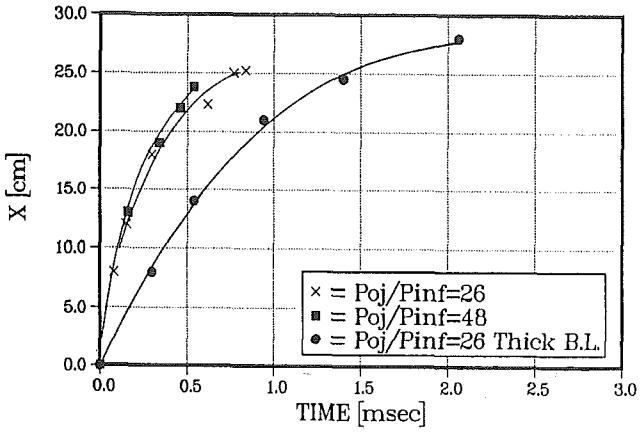

FIG 7. GROWTH OF THE INTERACTION ZONE : SEPARATION LENGTH VS. TIME.

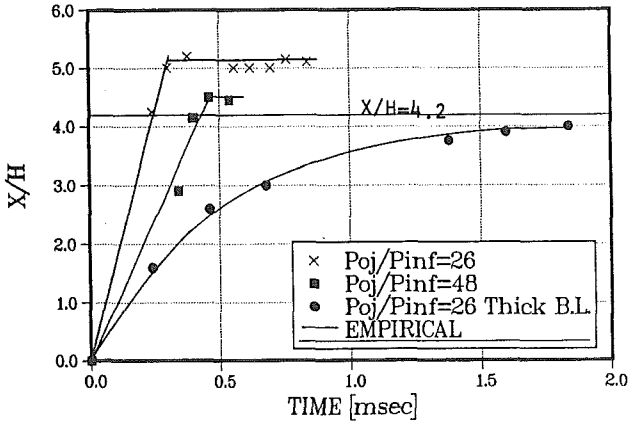

FIG 8. GROWTH OF THE INTERACTION ZONE : RATIO OF SEPARATION LENGTH/PENETRATION HEIGHT VS. TIME.

In conclusion, the undisturbed boundary layer properties do influence the rate of development of the interaction region. The experiments [5, 6] indicate that the interaction is influenced by the boundary layer thickness when this thickness is larger than the penetration height, which is clearly true in the last case examined. The present results also compare well with the experiments in that the ratio X/H for the fully developed flow is consistent with the empirically determined value of 4.2.

7. EFFECT OF FOREBODY SHAPE

Until now only flat plate results have been discussed. For real configurations it is necessary to consider shapes resembling flight vehicle forebodies. The elliptic shape has been chosen to represent configurations with detached bow shock, while the ogival shape represents those with attached bow shock. The treatment is still two dimensional, and the injection slot 1.2cm in width is located 15cm (5 body radii) from the body's origin. The computational grid (see Figure 9) is now composed of several blocks and is skewed and of variable density to best fit the flow topology.

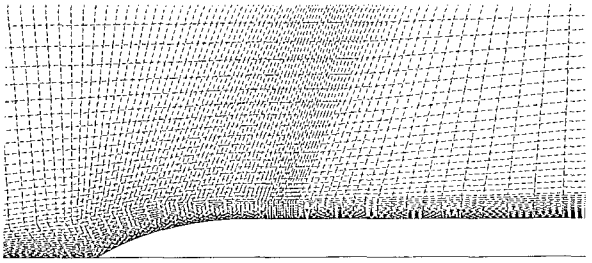

FIG 9. THE MULTIBLOCK GRID STRUCTURE.

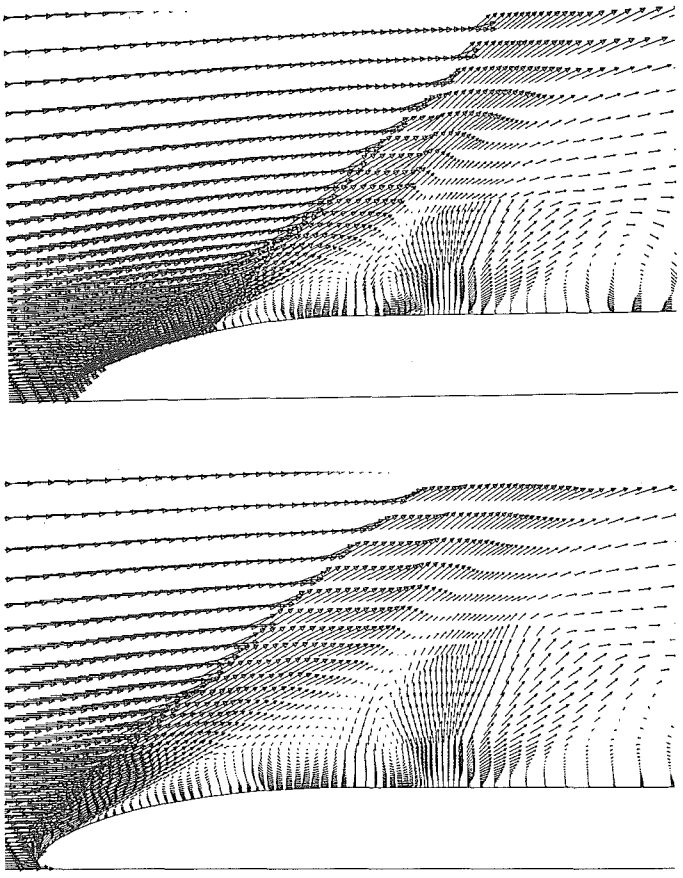

FIG 10. VELOCITY VECTOR PLOTS FOR OGIVAL (UPPER) AND ELLIPTIC (LOWER) FOREBODIES - Poj/Pinf=75, Minf=5

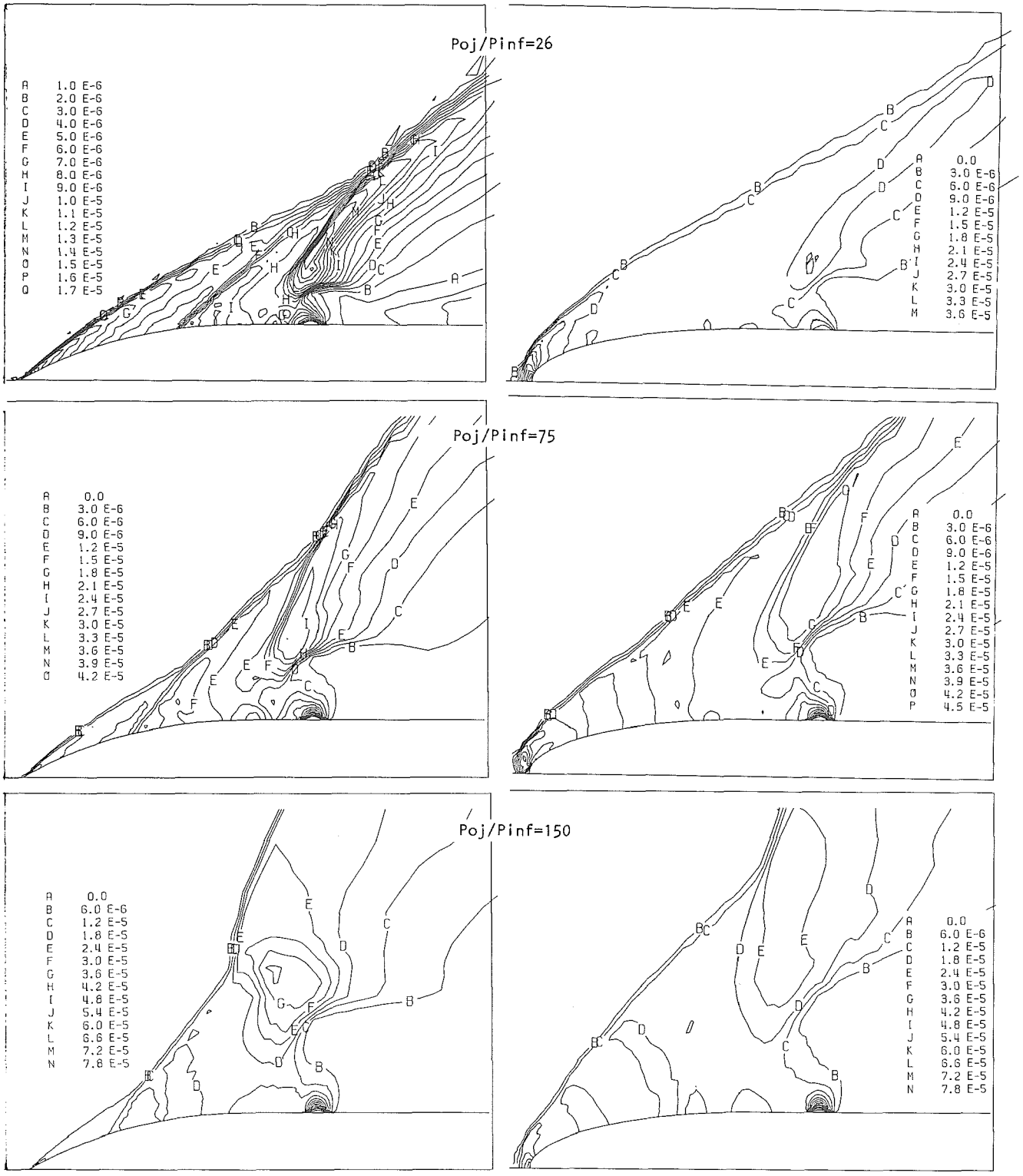

FIG 11. EQUAL PRESSURE CONTOURS FOR OGIVAL FOREBODY (LEFT) AND FOR ELLIPTICAL FOREBODY (RIGHT) FOR THREE INJECTION PRESSURE RATIOS. Minf=5

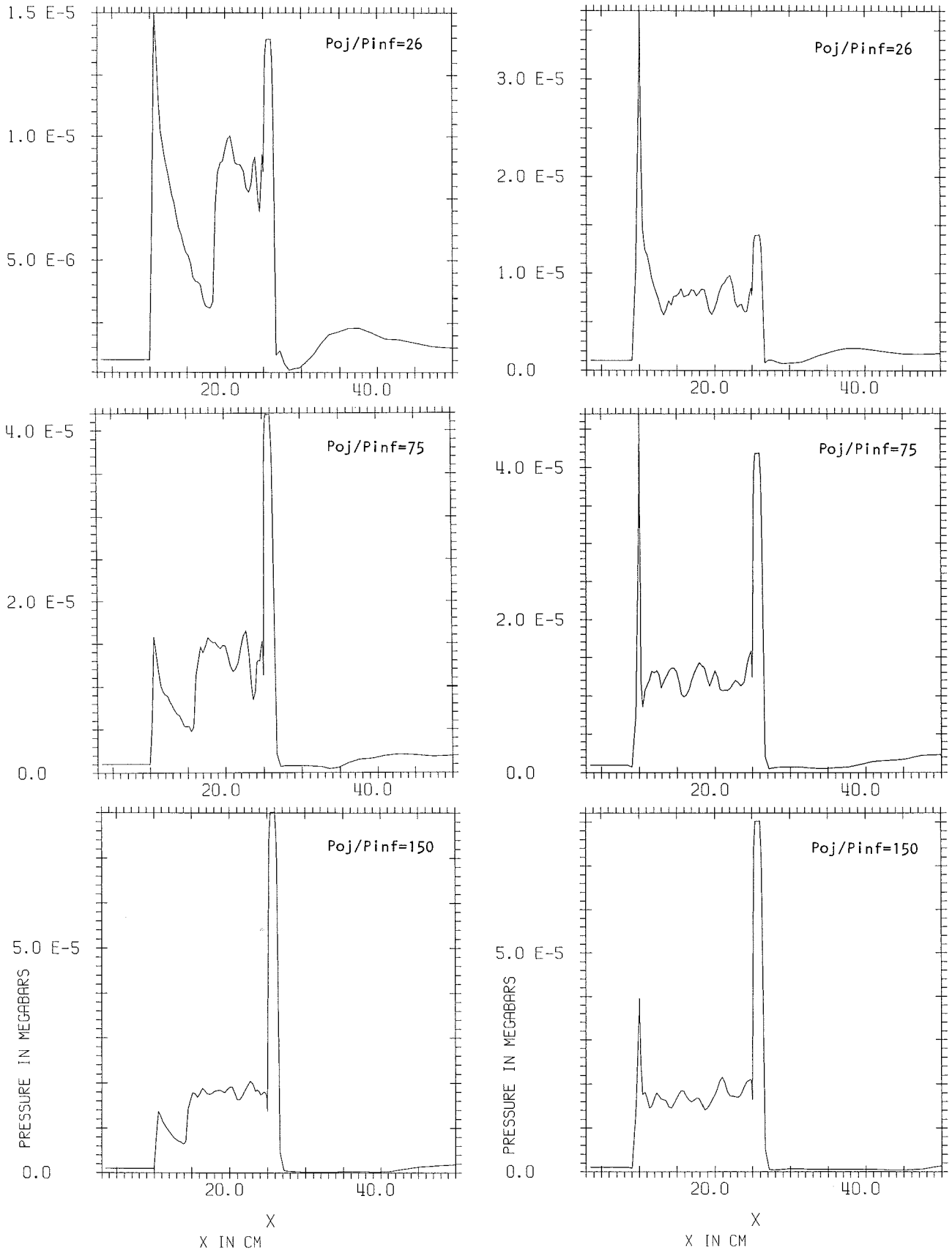

FIG 12. SURFACE PRESSURE PLOTS FOR OGIVAL FOREBODY (LEFT) AND FOR ELLIPTICAL FOREBODY (RIGHT) FOR THREE INJECTION PRESSURE RATIOS. Minf=5

The qualitative difference between the present configurations and the flat plate geometry is the interaction of the bow shock with the jet induced flow field present in the former case. It is therefore of interest to investigate how this interaction affects the force amplification. The control parameter for this study is the ratio Poj/Pinf. The values of the pressure ratio for which computations were carried out are: 5.7, 26, 75 and 150, and the Mach number was 5 for all the cases. The results of the simulations are plotted in terms of pressure contours, velocity field and surface pressures in Figures 10-12 for the ellipse and the ogive, respectively. The representative velocity vector diagrams for the case Poj/Pinf=75, is shown in Figure 10. It is to be noted that appearance of these plots is influenced by the grid nonuniformities and finite length of the arrows that originate at the cell centers. Perhaps the most revealing are the equal pressure contour maps (Figure 11), showing the complex interaction between the nose bow shock, the separation shock and the jet bow shock. The shock pattern is especially crisp for the ogival shape. For the highest injection pressure ratio, the jet bow shock forms an almost normal shock wave at its intersection point with the nose shock, for both configurations.

The surface pressure plots in Figure 12 are probable the best source of quantitative information. It is noted that separation region for the elliptic nose is consistently longer and the plateau pressures are higher, than for the equivalent ogive. For the ellipse with the detached bow shock the upstream separation zone reaches the forwardmost part of the body even for the lower values of the injection pressures. In contrast, the separation zone for the ogive does not reach the nose even for the highest value of the injection pressure. This is due to the basic differences in the flow downstream of attached and detached shock waves as well as with the surface geometry. For the ellipse, the flow exits the bow shock close to the surface at subsonic speed and has to go around a curved surface. It is therefore easier to separate than the flow over the ogive that is always supersonic and the curvature effects are relatively small. The plateau pressures are now a strong function of the injection pressure - as will be recalled, for the flat plate the dominant factor was the free stream Mach number.

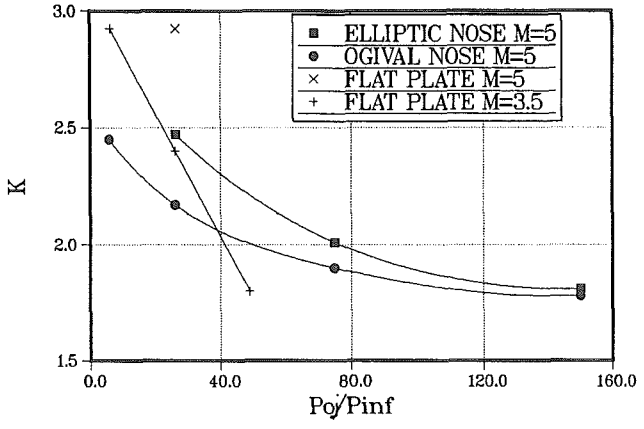

FIG 13. VARIATION OF THE AMPLIFICATION FACTOR WITH PRESSURE RATIO FOR THE DIFFERENT FOREBODY SHAPES.

The three-dimensional computations of Shang et al. [1] show basically similar surface pressure distributions. This is encouraging, since it indicates that the present, planar results may be valid for general, three-dimensional configurations, as has been hoped. Shang et al. [1] did not observe significant differences between sharp and blunt body for their single comparison using much weaker injection. It is expected that for stronger injection the findings would parallel the present results.

The influence of the bow shock on the jet interaction may perhaps be explained by drawing an analogy between the shock and a retaining wall. Thus, the zone of upstream influence is limited and consequently the pressures are higher than for an unconstrained (flat plate) case. The surface pressures have been integrated and are displayed, as before, in the form of characteristic interaction parameters in Table 5. It is interesting, and perhaps surprising, that the amplification factor is similar in magnitude for both configurations, though larger for the ellipse (detached shock). These results are quite similar to the flat plate results as seen in the comparison plot in Figure 13. The amplification factor, K, appears to become insensitive to injection pressure for large values of the pressure ratio.

The present comparisons were limited to pressure ratio (Poj/Pinf) of 150. Up to this value no blow-off of shock wave was obtained. It would be of great interest to investigate the interaction flow field for larger values of injection pressures to see if and when blow-off occurs.

FOREBODY	Poj/Pinf	Fi/T	K
ELLIPTIC	JET OFF	-	-
ELLIPTIC	26	1.49	2.47
ELLIPTIC	75	1.01	2.01
ELLIPTIC	150	0.83	1.81
OGIVAL	JET OFF	-	-
OGIVAL	5.7	1.60	2.45
OGIVAL	26	1.23	2.17
OGIVAL	75	0.91	1.90
OGIVAL	150	0.78	1.78

TABLE 5. INTERACTION PARAMETERS FOR THE TWO FOREBODY SHAPES. SEA LEVEL, Minf=5

8. CONCLUSIONS

A parametric, numerical study of the jet interaction phenomenon was presented. First, the sonic jet injected transversely through a slot in the flat plate was examined. It was shown through detailed comparison of a test case with available experimental data, that the present simulations faithfully reproduce the flow field topology as well as the surface pressures in the interaction zone. Having established that, the influence of various parameters on the jet interaction flow field was studied. Unlike other published numerical works, the emphasis here was placed on the various interaction parameters, such as the amplification factor, that are a reflection of

the magnitude of the force available for flight vehicle control. It was found that increasing the injection pressure decreases the force amplification because the overexpansion of the jet decreases its relative penetration height. Increasing the Mach number was found to increase the interaction force, while the experiments appear to show insensitivity to that parameter. Because of large scatter of the experimental data, it is hard to judge this discrepancy. Vectoring the jet in the upstream direction increased the interaction force significantly for smaller jet pressure ratios.

Simulations were also carried out with the jet replaced by a wall (spoiler) and the expected analogy between the two flow fields was demonstrated. It was shown that, unlike the jet, the spoiler carries with it a drag penalty significant in magnitude when compared with the effective control force.

Advantage was taken of the time-dependent nature of the present solution to study the transient during which the jet interaction flow field is formed. The time scale for establishing the interaction flow field is the same as the time needed for the outer flow to traverse this length, for boundary layers that are thinner than the penetration height of the jet.

The effect of ogival and elliptical forebody shapes having attached and detached shock waves, on the jet interaction was studied. The shock significantly affects the jet induced flow field, but the force amplification factors were surprisingly similar to the flat plate results. The bow-wave acts essentially like a retaining wall, limiting the upstream spread of the interaction zone, but increasing the pressures within the region.

The present results and conclusions are strictly valid for planar flow. However, qualitatively at least, these results should be indicative also for the general three-dimensional configurations. This was shown true by several comparisons with three-dimensional computations.

In addition to the cases presented in this paper, cases with hot gas injection and different species injection were also computed. Results often indicated long, unstable shear layers, and multiple recirculation cells were present. Steady-state solutions were not always obtained, especially when the separation region was extensive. Further work in this area is needed. It is also planned to extend this work into an experimental stage. This will provide a data base for various generic but realistic configurations. It would also be of interest to find out to what extend can the conclusions reached on the basis of two-dimensional numerical simulations be carried over to actual three-dimensional configurations.

REFERENCES

1. Shang, J.S., McMaster, D.L., Scaggs, N. and Buck, M., "Interaction of Jet in Hypersonic Cross Stream", AIAA Journal, Vol.27,No.3, March 1989, pp.323-329.

2. McMaster, D.L., Shang, J.S. and Golbitz, W.C., "Supersonic, Transverse Jet from a Rotating Ogive Cylinder in a Hypersonic Flow", Journal of Spacecraft, Vol.26,No.1,Jan.-Feb. 1989, pp.24-30.

3. Lombard, C.K., Hong, S.K., Bardina, J., Codding, W.H. and Wang, D., "CSCM in Multiple Meshes with Application to High Resolution Flow Structure Capture in the Multiple Jet Interaction Problem", AIAA Paper 90-2102, 26th. Joint Propulsion Conference, Orlando, FL, July 16-16 1990.

4. Hong, S.K., Bardina, J., Lombard, C.K., Wang, D. and Codding, W.H., "A Matrix of 3-D Turbulent CFD Solutions for JI Control with Interacting Lateral and Attitude Thrusters", AIAA Paper 91-2099, 27th. Joint Propulsion Conference, Sacramento, CA, June 24-26, 1991.

5. Spaid, F.W., "Two-Dimensional Jet Interaction Studies at Large Values of Reynolds and Mach Numbers", AIAA Journal, Vol.13,No.11, November 1975, pp.1430-1434.

6. Spaid, F.W. and Zukoski, E.E., "A Study of the Interaction of Gaseous Jets from Transverse Slots with Supersonic External Flows", AIAA Journal. Vol.6,No.2, February 1968, pp.205-212.

7. PISCES 2DELK Versin 4, Physics, Int., San Leandro, CA/Gouda, The Netherlands.

8. Zukoski, E.E., "Turbulent Boundary Layer Separation in Front of a Forward Facing Step", AIAA Journal, Vol.5 ,No.10, October 1967, pp.1746-1753.

9. Baranovsky, S.I. and Schetz, J.A., "Effect of Injection Angle on Liquid Injection in Supersonic Flow", AIAA Journal, Vol.18,No.6, June 1980, pp.625-629.